Behavior of Flexible Pavements on Expansive Soils

Adel Djellali[1], Abdelhafid Ounis[2], Behrooz Saghafi[3]

Abstract:

This investigation discusses the findings on analysis results of a pavement structure constructed on a relatively expansive material consisting mainly of brown clayey silt in Tebessa, Algeria. Cores were brought to the laboratory from a piece of roadwork. Remolded samples were taken from subgrade of a deteriorated road. The soils were generally found to be of medium plasticity and of a medium to high expansion potential. Oedometer test for free swell indicated a constant volume pressure that produced stress in excess of 350 kN/m2. The following involves describing the behavioral characteristics of expansive soil as it relates to flexible pavements. Soils are generally classified using the X-ray diffraction [XRD]. Computer code Plaxis 8.2 was used for numerical simulation to check the behavior of structure pavement with three models in pavement structure, and free expansion test was performed to calibrate the soil subgrade with Soft-Soil model. The study is based upon simulating the vertical subgrade soil displacement during traffic load, and its influence on load-settlement on flexible pavement behavior. To stabilize the swelling character of subgrade, an adequate surcharge pressure is used according to the procedure described in the article.

Keywords: Flexible pavements; expansive subgrades; soil calibration; Oedometer test; Soil behavior; Finite element method

Corresponding author Email: adel1830@yahoo.fr.

1. Assistant Professor, Department of Civil Engineering and Hydraulics, University of Mohamed Khider, Biskra, Algeria
2. Assistant Professor, Department of Civil Engineering and Hydraulic, University of Mohamed Khider, Biskra Algeria
3. Assistant Professor, Tarahan Parseh Transportation Research Institute, Tehran, Iran

1. Introduction

Several pieces of pavements can be found on expansive soils in many parts of the world, particularly in semi-arid regions. Such soils are generally unsaturated and contain a large amount of clay. Expansion of the clayey soils, containing smectites or illites in varying quantities, is the root cause of numerous distresses in buildings and large structures [Baheddi et al., 2007]. In the presence of water after a dry state, these soils undergo a significant volume change. The volume change of expansive soils is primarily due to the hydration of the clay minerals or more precisely, the adsorption of water molecules to the exterior and interior surfaces of clay mineral to balance the inherent change deficiency of the particle [Snethen et al., 1975]. Contrary, if the soil is parched, it undergoes a reduction in volume, i.e. shrinkage takes place, which leads to the development of network cracks of polygonal shapes. They are manifested by intense degradation of pavements and surrounding grounds. The losses due to extensive damage to highways running over expansive soil subgrades are estimated to be in billions of dollars all over the world [Prasad et al., 2010; Jones and Holtz, 1973]. Various remedial measures like soil replacement [Snethen et al., 1975], pre-wetting [SubbaRao and Satyadas, 1980], moisture control [Marienfeld and Baker, 1999] and lime stabilization [Thompson and Robnett, 1976] have been practiced with varying degree of success. However, these techniques suffer from certain limitations respect to their adaptability, like longer time periods required for pre-wettting the highly plastic clays, [Steinberg, 1977; Felt, 1953], difficulties in constructing the ideal moisture barriers [Snethen et al., 1975], pulverization and mixing problems in case of lime stabilization [Ramana Murty, 1998] and high cost for hauling suitable refill material for soil replacement [Chen, 1988; Snethen et al., 1975], geogrids reinforcement [Guptaet al., 2008], polymer grid reinforcement [Miura et al., 2003], geosynthetic reinforcement [Zornberg and Gupta, 2009], Polymer grid [Miura et al., 2003], etc.

The problem is further exacerbated when the subgrade is expansible. Even if the pavement is correctly designed, the swelling character of the subgrade goes to distort all predictions. It is well known that larger stresses can be created when volume change of a material occurs. The stresses reflect in the form of cracking, heaving and settlement of highway pavements. Therefore, a significant increase in the costs of routine maintenance, rehabilitation and even reconstruction of the deteriorated pavements will be forced to the road authorities [Hyunwook and William, 2009]. The cracking phenomenon can occur through volumetric changes under changing moisture conditions in expansive subgrades. These volumetric deformations usually result in differential movements of flexible pavements resting on the expansive subgrade. Consequently, structural damages could happen if no special measures have already been taken during the design process [Ayman, 2007].

The method used for pavement design in Algeria is known as the-catalog structure and is based on the French Method that uses the elastic Burmister's model for a multi-layer, semi-infinite structure. It assumes a semi-analytical stress-based field where deformations are calculated for when pavement is subjected to very heavy traffic. However, in the case of flexible pavement over expansive soils, subjected to high gradients of volume change, the method does not take into account such an effect in predicting pavement behavior. Literature reveals that several locations in Tebessa, Algeria, are made of expansive soils causing pavement deteriorations. As a part of road network maintenance, rehabilitation methods have been developed specifically for the flexible pavements of a National Highway [N10], which has suffered from severe degradation in its structural integrity. The geotechnical records of N10 show that it was constructed on expansive subgrades. Totally, 31 soil samples were taken, 10 of which were core samples and 21 were from wells. The results of laboratory test classified these soils of having medium to high expansion potential. Further soil data were obtained using the Principal Component Analysis [PCA]. Plaxis 8.2 software package with its linear elastic, Mohr Coulomb and soft soil models were used to predict soil variations. A surcharge pressure was used to stabilize the heave of the pavement structure.

2. Location of The Study Area

Flexible pavement on expansive soils is generally common in Tebessa, Algeria. The city consists of a collapsed basin surrounded by mountains, with an average

altitude of 800 to 1600 m above mean sea level. The city is bounded from north by the city of Souk-Ahras, from south by El'Oued, from east by the Tunisian border and from west by two cities OumEl-Bouaghi and Khenchella, with an area of 21,000 km2. The 4.5 km long highway commences at the intersection of N10 and N82 [El Kouif road] and ends at the intersection of the N16 [El Malabiod road] and road of Bekkaria, with an average altitude between 814 and 842 meters above mean sea level [Figure.1].

3. Classification and Soil Profile at The Test Site

As a part of enhancing the mechanical behavior of National Highway N10, a soil testing program was set up to test 10 trials of the samples cored 6 m deep and 21 wells of 2 to 3 m deep using a shovel. The purpose was to establish the geological profile of the site and to ensure there were enough intact and disturbed samples for laboratory testing. Visual analyses of wells and core samples revealed the presence of marly clay, clayey silt and marl. Table 1 shows the geotechnical characteristics of samples. Classification by Casagrande chart [Atterberg Limits] – based on liquid limit LL and plastic limit PL – showed that these soils were inorganic clay with medium to high plasticity. Another classification with Dakshanamanthy and Raman [1973] – based on

same parameter of Casagrande chart for the expansion potential – showed that the expansion potential of the soils was medium to high [Figure.2]

In addition to the routine characterization testing, the X-ray diffraction [XRD] technique was used to obtain semi-quantitative mineralogical composition and chemical analysis [Saad and Aiban, 2006]. We have used PANalytical X'Pert PROX-Ray Diffractometer [Type MPD] to obtain the data. These XRD micrographs vividly confirmed that soils are marly clays with 64% of calcite and 35% of aluminosilicate [Figures. 3].

4. Calibration of Oedometer Test For Free Swell

One-dimensional tests are instrumentals for predicting the compressibility, collapse and expansion potential of soils [Saad and Aiban, 2006]. A geotechnical investigation company issued the permission of extracting undisturbed samples from the depths of 0.3 – 3.0 m and 3.0 – 6.0 m for oedometer test for free swell.

The results of testing were used in a calibrated soft soil model programmed in computer code as Plaxis 8.2. With respect to the geometry of the test, oedometer cell is simulated using a plane strain model by elements containing 15 nodes. For 10 trials of swelling pressure, the intention was to reach as closely as possible to the
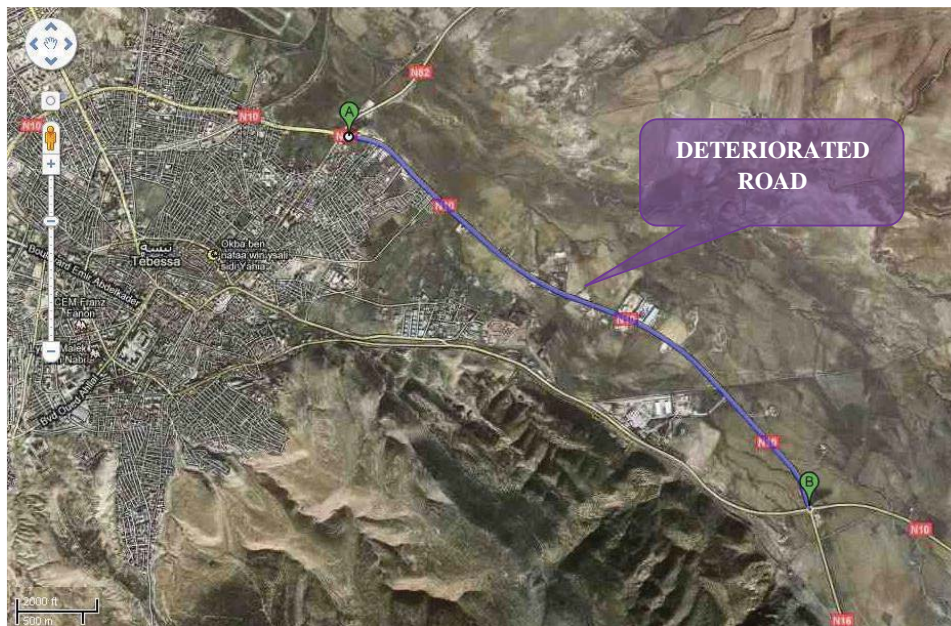

Figure 1.Satellite view of Tebessa with indication of the modelled area [Google map].

Table 1. Basic geotechnical and swelling characteristics of the samples.

| Sample N°	Depth [m]	elements <0.08mm %	Moisture content, W%	Dry density γ_d kN/m³	Wet density γ_h kN/m³	Liquid limit, LL%	Plasticity index, PI%	MB cm³/g	Caco3 %	Swell pressure kN/m²
1	1.18-2.00	93.4	19.36	1.56	1.82	63	38	7.3	48.38	-
2	1.30-2.00	92.4	19.26	1.56	1.84	64	36	7.8	51.38	-
3	0.25-2.00	92.4	18.36	1.56	1.86	64	37	7.8	48.36	-
4	0.30-2.00	98	14.26	1.52	1.82	62	36	7.2	49.38	-
5	0.30-2.10	92	12.89	1.70	1.86	52	32	7.1	59.38	-
6	0.30-2.00	93.6	8.37	1.49	1.64	34	16	2.0	73.55	-
7	0.20-2.00	97.6	12.82	1.71	1.88	50	30	7.1	60.26	-
8	0.20-3.00	97.6	12.71	1.70	1.89	51	31	7.0	60.00	-
9	0.30-3.00	97.2	12.84	1.72	1.87	48	32	6.9	59.38	-
10	0.20-1.50	96.4	12.6	1.70	1.86	52	32	7.18	46.28	-
11	0.70-2.30	97.6	18.33	1.47	1.75	65	39	7.17	46.15	-
12	0.25-1.50	95.6	12.76	1.70	1.86	50	30	7.2	59.36	-
13	0.25-2.00	97.2	12.36	1.71	1.88	51	32	7.0	58.86	-
14	0.30-2.00	96.8	12.38	1.72	1.90	50	31	7.26	59.42	-
15	0.30-2.00	97.4	13.34	1.72	1.91	52	33	6.82	64.36	-
16	0.30-3.00	97.2	12.89	1.73	1.99	58	36	6.84	47.26	-
17	0.20-3.00	96.8	15.85	1.70	1.98	59	38	6.83	45.38	-
18	0.40-2.00	96.8	14.25	1.72	1.96	58	37	6.26	46.34	-
19	0.40-3.00	96.6	12.65	1.71	1.93	47	28	5.67	44.62	-
20	0.70-1.40	45.18	14.5	1.72	1 .95	34	14	4.5	61.48	-
21	0.68-1.00	98.25	18.6	1.66	1.97	52	30	6.5	44.44	-
22	0.50-6.00	91.6	27.66	1.48	1.89	50	31	4.11	49.61	200
23	0.70-2.50	97.8	17.53	1.71	2.01	56	36	6.3	53.48	240
24	0.50-3.00	98	17.24	1.70	2.01	53	31	3.95	63.33	280
25	0.40-4.00	93.8	19.39	1.63	1.99	59	42	7.8	42.76	350
26	0.50-5.00	92.4	26.60	1.47	1.86	58	37	7.14	45.59	300
27	0.60-5.50	93.4	19.83	1.70	2.03	41	40	7.3	48.78	340
28	0.40-2.40	92.6	19.84	1.56	1.86	51	33	7.8	40.00	320
29	0.40-3.00	93.8	27.72	1.56	1.95	52	33	5.9	62.20	175
30	0.50-5.00	98.6	17.74	1.58	1.85	46	30	6.0	50.00	240
31	0.70-6.00	98.6	23.06	1.60	2.04	53	35	6.1	53.97	240
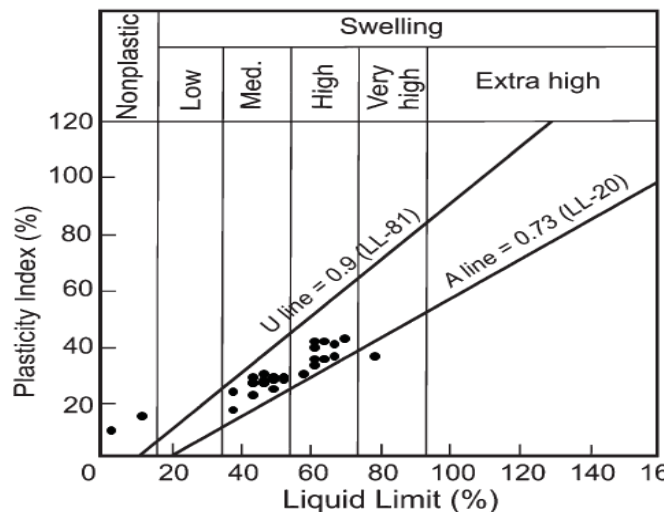
Figure 2.Classification of subgrade soils of Tebessa, based on Dakshanamanthy and Raman [1973]
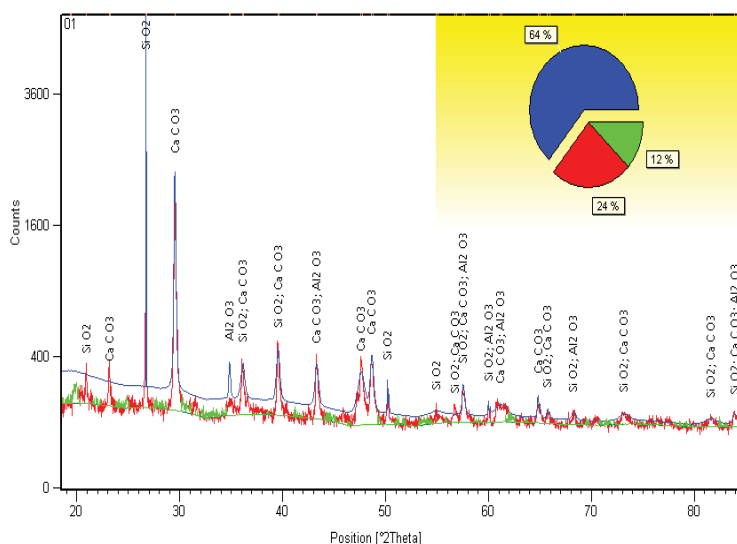
Figure 3.[a].XRD result of sample n°15 [bleu: calcite, red: silica, green: alumina]
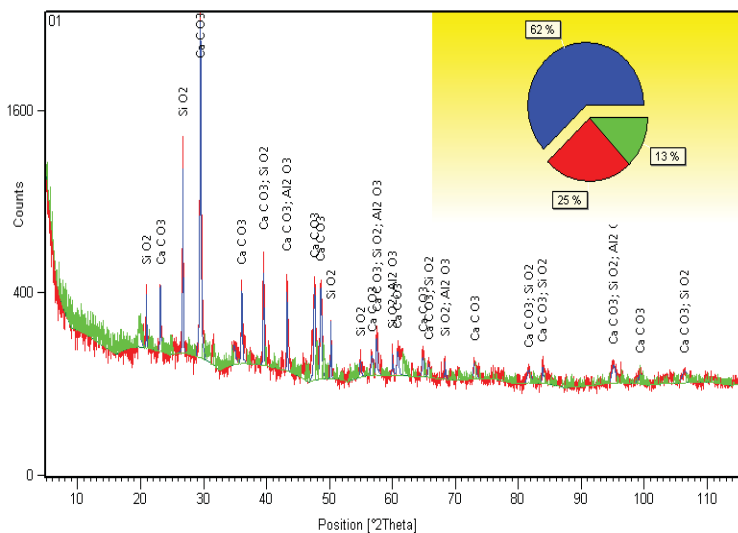

Figure 3.[b]. XRD result of sample n°29 [bleu: calcite, red: silica, green: alumina]

real parameters seen in site. Initial values given to the soil parameters were γ_n=18.3 kN/m³, γ_{sat}=21.1 kN/m3 and permeability of 0.001 m/day in undrained conditions. Shear strength parameters were taken directly from the C.U test [direct shear test] which released φ=8° and C=75 kN/m2 with a dilatancy angle of Ψ=0°. Oedometerparameters are taken directly from the oedometer test results, the modified compression index $\lambda^* = Cc/2.3[1+e]$=0.036 and the modified swelling index $\kappa^* = 2Cg/2.3\ [1+e] = 0.035$. Void ratio was e=0.47. All these parameters are essential for the model. A large number of calculations have been followed by changing the value of the parameters between their

lower and upper bounds. The results have been summarized in Table 2.

Figure.4 shows the results of the curves of expansion pressure; the variation of $\Delta H/H$ versus log $[\sigma]$. The real curve [RC] has been compared with the numerical curve, which has been resulted from simulation. The calibration results allow for a good simulation of both the initial small strain stiffness and of the large strain behavior. The user-defined function of Plaxis was used in order to set the pore water pressure distribution so that it simulates the expansion pressure for the calibration process.

The numerical simulation of free expansion test re-

Table 2. Combination of parameter for calibration.

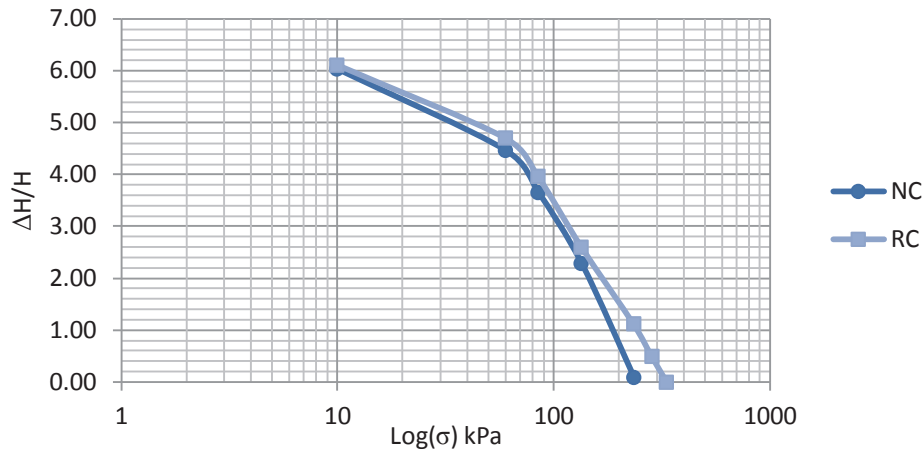| Parameter	Upper bound	Lower bound	Number Of steps	Selected value
Cc	0.100	0.800	70	0.290
Cg	0.020	0.100	45	0.072
C[kN/m²]	10	100	45	82
󠀠󠀠󠀠󠀠󠀠	1	25	25	4.4

Figure 4.Simulation of free swell test for the sample at the depth of 3 m [RC: real curve; NC: numerical curve]

vealed a value of 240 kN/m2 instead of 340 kN/m2 obtained from the real test. Similar deformations were observed in the first four loading levels. All these validate that the free expansion test overestimates the expansion pressure in the case of medium to highly expansive soils, since the free-swelling test can cause changes in structure during expansion before it returns to the zero strain state, where this state was also seen by Bultel [2001].

5. Numerical modeling
5.1. Objective
In order to cope with the complications of describing the swelling behavior of the expansive soil, researchers have developed alternative approaches [Banu et al., 2009]. One of them being the use of finite elements, the main purpose of finite element simulation is to:

1. Get a deeper understanding as to why permanent deformations happen in different parts of flexible pavements resting on expansive soils;

2. Find the best method to model the stresses. Since the stress state depends on the soil model, several kinds of material models have been tested to estimate which soil model would give the most reliable stress distribution. This stress-strain analysis created a basis platform for

future development of models in permanent deformation;

3. Find the stabilization methods to overcome the cycling variations of expansive subgrade.

Plaxis version 8.2 was used to model the behavior. Pavement structures have rarely been analyzed with finite element programs under dynamic loading. One reason for this is the fact that traffic loading is much more complicated than static loading normally applied in geotechnical problems. Another reason is that the material models in finite element programs have mainly been developed for static loadings not for repetitive cyclic loading. Dynamic analysis needed to be tested with a repetitive half-sin loading; but it was found that the dynamic module of Plaxis 8.2 was not suitable for modeling the traffic loading [Leena, and Rainer, 2004]. Given the aforementioned reasons, the analysis has to be simplified. The first part of the expansion pressure analysis was to study the volumetric changes of the subgrade by the test oedometer for free swell. With this analysis, the subgrade calibration was based on physical and mechanical parameters such as cohesion [C], friction angle [φ], density and oedometer parameters of Cc, Cg and Pc. To approach as closely as possible to the actual state, a large-scale numerical model, which

includes a flexible pavement structure based on an expansive subgrade, was established. The structure was subjected to the loads from two trucks with dual wheel load of 650 kN/m2 per axle. Then a complete analysis of stress-strain was performed on the pavement structure.

5.2. Modeling

Modeling was to simulate an existing flexible pavement structure that had suffered several damages after one year of its construction. This road had been constructed on an expansive subgrade classified as brown clayey silt. The total thickness of the pavement was 0.76 m. Clayey silt subgrade was covered with a 0.20 m layer of calcareous tufa as the improved subgrade, 0.20 m crushed gravel as subbase course, 0.20 m crushed gravel as base course and 0.06 m asphalt on top. The distresses observed on the pavement can be summarized as mild transverse and longitudinal cracks, mid-block cracking, alligator cracking along the shoulders, consolidation rutting for 0.06 m deep and finally average subsidence. A form of cracking can be seen in Figure. 5. Oedometer test for free swell showed that the vertical deformation [uplift] has a maximum height of 0.021 m with 350 kN/m2 of expansion pressure. The groundwater level fluctuated between 0.00 and 0.50 m. No change in water pore pressure was considered for hydraulic analyses.

At first, passage of just one truck was simulated. Then, loading from two trucks at the same time with dual wheel of 0.60 m wide was studied. Modeling was done by a static ax-symmetric analysis and the element mesh consisted of triangular elements each with 15 nodes. The input parameters of the structure are shown in Table 3. To simulate the variation of stresses dependant on the Young's modulus, layers were divided into sub-layers with the same strength parameters but with different elasticity modulus. Use of plain-strain analysis, where the loading would have been continuous linear loading, could result in an overestimation of stresses and responses [Leena and Rainer, 2004]. To model the loading area of the dual wheel, the total load was transferred to a circular load with a known mean contact pressure. The detail of the structure and boundary conditions are illustrated in Figure. 6.

For this model, the attention was focused on the stresses and resilient deformations. The modeling initiated from values derived from the laboratory tests. The results of measurements and calculations of the resilient deformations were compared with each of other soil parameters and they were modified to provide a distribution of stresses and strains as close as possible to the reality, i.e. the calibrated soil that has been mentioned previously.

The magnitude and development of permanent deformations depend on static stress state of the material [Žlender, 2008], and how far the stress state is from the static failure line. This assumption is not entirely valid in the case of traffic load, but it gives a good estimate about sensitivity of materials for permanent deformation. The static failure criterion, where it is widely adopted in geotechnical and in pavement materials, is
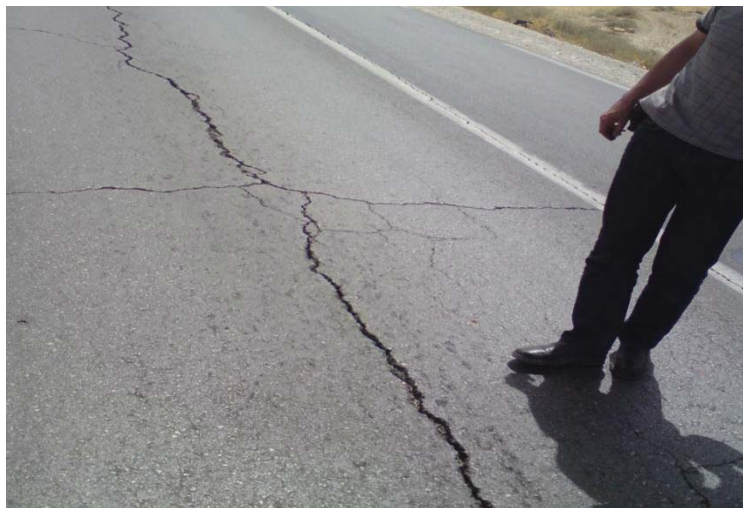

Figure 5. Cracking distress on pavement structure.

Behavior of Flexible Pavements on Expansive Soils

Table 3. Input parameters of the model.

Material	Asphalt	Base course crushed gravel	Subbase crushed gravel	Improved subgrade tufa	Subgrade swelling clay
Thickness, mm	60	200	200	200	2000
Young's Modulus, MN/m^2	5400	300–200	140–90	70	10–8
Poisson's ratio	0.35	0.35	0.35	0.25	0.35
Unit weight, kN/m^3	25	21.2	22.0	20	18
Cohesion, kN/m^2	--	30	20	9	10
Friction angle [°]	--	43	44	36	25
Dilatation angle [°]	--	13	14	6	0
K_0	1	0.32	0.30	0.4	0.8
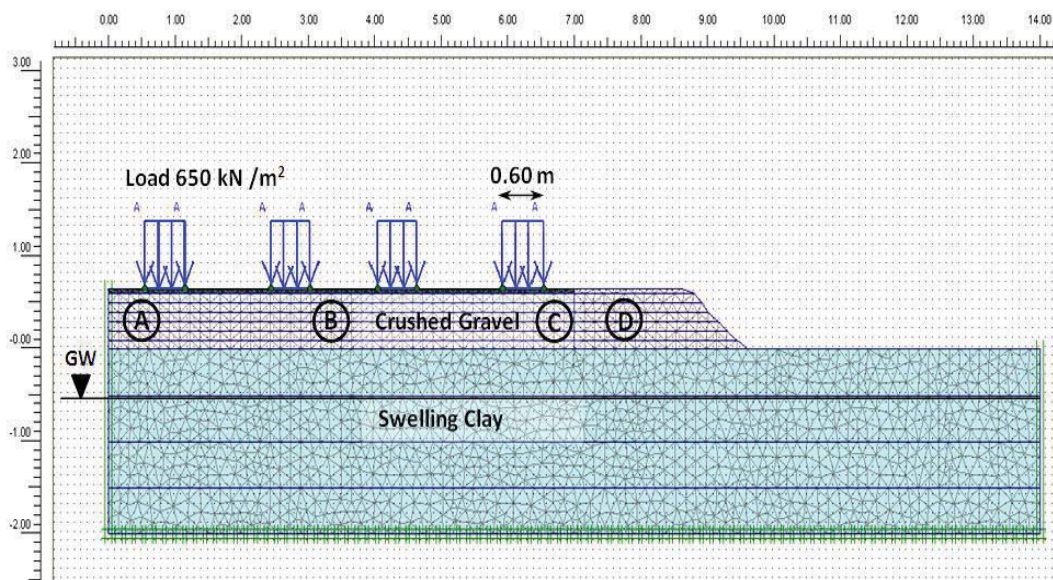
Figure 6. Numerical model: details and the boundary conditions

with the failure criterion of Mohr-Coulomb [Leena and Rainer, 2004]. However, the experimental results show that the strength envelopes of almost all geo-materials have the nature of nonlinearity in the σn–τ stress space. In addition, linear failure criterion is a special case of failure criteria [Lianheng et al., 2010]. The behavior of embankment connects the failure ratio to the deviatoric stress ratio, in this case the failure ratio R can be written as follows:

$$R = \frac{q}{q_0 + Mp'};$$ (1)

where $M = \frac{6.sin\emptyset}{3 - sin\emptyset}$ and $q = \frac{c.6.cos\emptyset}{3 - sin\emptyset}$

R   the failure ratio
q   deviatoric stress, kN/m2
q0   deviatoric stress, when p' = 0

C   Cohesion, kN/m2
M   the slope of the failure line in p'-q space
p'   hydrostatic pressure, kN/m2
φ   friction angle.

Since the subgrade has a swelling character, it was modeled by Soft-Soil model. This model takes into account the following parameters: stress dependent stiffness [logarithmic compression behavior], distinction between primary loading and unloading cycle [compatible with the swelling behavior], memory for preconsolidation stress and failure behavior according to the Mohr-Coulomb criterion [Brinkgreve, 2002]. The Soft-Soil model assumes that there is a logarithmic relationship between volumetric strain [ε_v] and mean effective stress [p'], where the virgin compression can be formulated as:

$$\varepsilon_v - \varepsilon_v^0 = -\lambda^* ln\left(\frac{p'}{p^0}\right) \tag{2}$$

where λ^* is the modified compression index and ε_v^0 is the initial volumetric strain.

During isotropic unloading and reloading a different path [line] is followed, which can be formulated as:

$$\varepsilon_v^e - \varepsilon_v^{e0} = -\kappa^* ln\left(\frac{p'}{p^0}\right) \tag{3}$$

where κ^* is the modified swelling index [Brinkgreve, 2002].

6. Analysis of Results

The modeling results have been presented in Figure. 7 and 8. Three material models were applied, such as linear elastic model, Mohr-Coulomb and Soft-Soil model. Linear elastic model was the first model for calculations, which look into the pavement structure and subgrade in its entirety. In the modeling, the modulus of each layer was tested as described earlier and then fixed to some practical values. Mohr-Coulomb model used the same deformation parameters in linear elastic model, along the subgrade and pavement structure. Finally, the pavement structure was modeled by Mohr-Coulomb model and subgrade with Soft-Soil model. The stress states of the subgrade in three models and the analysis of the structure, as illustrated in Figure.7, indicate where the plastic, tension-cut-off and cup points are situated in structure with the same calculations.

Figure. 7 shows the plastic points in subgrade and pavement according to the three models. For the linear elastic model, it shows no presence of plastic points, for Mohr-Coulomb model. It is observed that the subgrade is largely affected by tensile cut-off points, in upper part of the pavement and shoulders, with the appearance of plastic Coulomb points in transition zone between the pavement and shoulder and in contact with traffic loads. For the Soft-Soil model, concentration of cap points in the subgrade under the shoulder and middle width of the pavement, concentration of tensile stresses [tension cut-off] in shoulders and in surface course, concentration of plastic Coulomb's points in contact between wheel and pavement and in the transition zone between the pavement and shoulder are clearly seen.

Figure. 8 illustrates total displacements in the subgrade and pavement by three models after two cycles of loading. The Figure depicts that according to the first two models, i.e. linear elastic where the total displacements are 1.65 x 10⁻³ and Mohr-Coulomb model with maximum displacements of 1.79 x 10⁻³ m, displacements in the pavement occurred only in the contact between wheels and surface course while they do not affect the subgrade. On the other hand, it was evidenced in the Soft-Soil model results that the movements had concentrated largely in subgrade beneath the transition zone between the pavement and shoulders and along the left side of the road where the pavement is slightly deformed with maximum displacements of 44.26x10⁻³ m.

Figure. 9 represents the curves of stress path for subgrade and surface pavement, and it reveals that the subgrade [of expansive clay] has elasto plastic hardening behavior, and the pavement has an elasto plastic nonlinear behavior with a various moduli of deformation along different parts of pavement. Figure. 10 represents the vertical displacement of subgrade and pavement structure. It shows that movements of swelling subgrade affect different parts of pavement, where points A, B, C and D are located in the pavement structure as shown in Figure. 6

## 7. Stabilization by Surcharge Pressure

One of the following methods provides the calculated surcharge pressure: (1) constructing an inert embankment to a calculated height and [2] replacing the existing soil to a calculated depth with inert material; the combination of the two methods can also be utilized.

To overcome the distress of pavement over expansive subgrades and to limit their heaves, the subgrade is loaded by a surcharge pressure equal to the swelling pressure. The principle is to make equilibrium between the pavement structure and the subgrade by eliminating the upward swelling pressure. This can be done by applying a surcharge on the subgrade (Figure. 11). The surcharge pressure is designed within a two-stage procedure, replacing a part of the current subgrade with a non-expansive material and heightening the embankment so much that the desired surcharge pressure is obtained. The goal is to obtain equilibrium as a result of which the swelling pressure is eliminated and cyclic
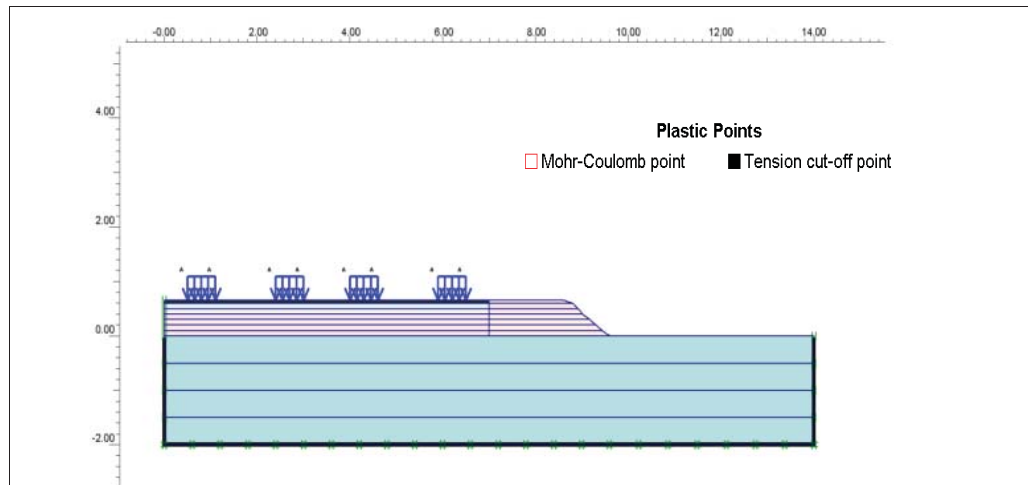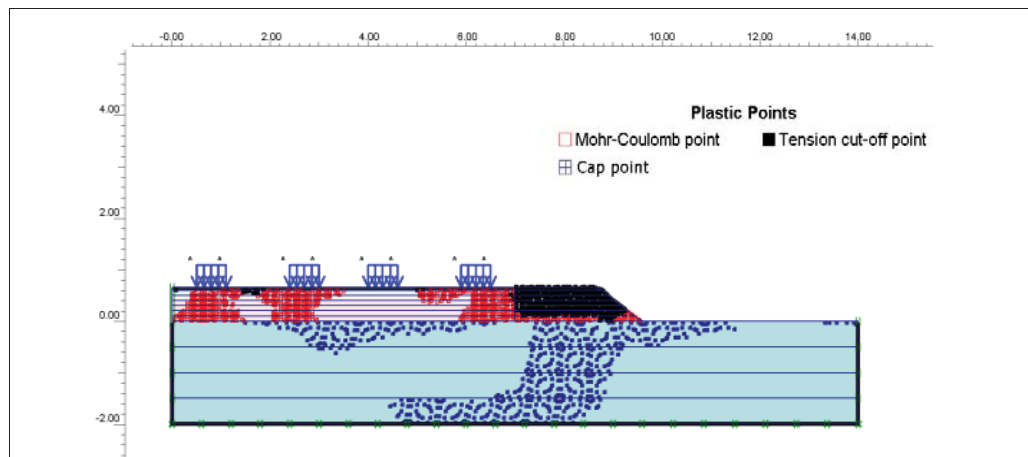
Linear elastic model
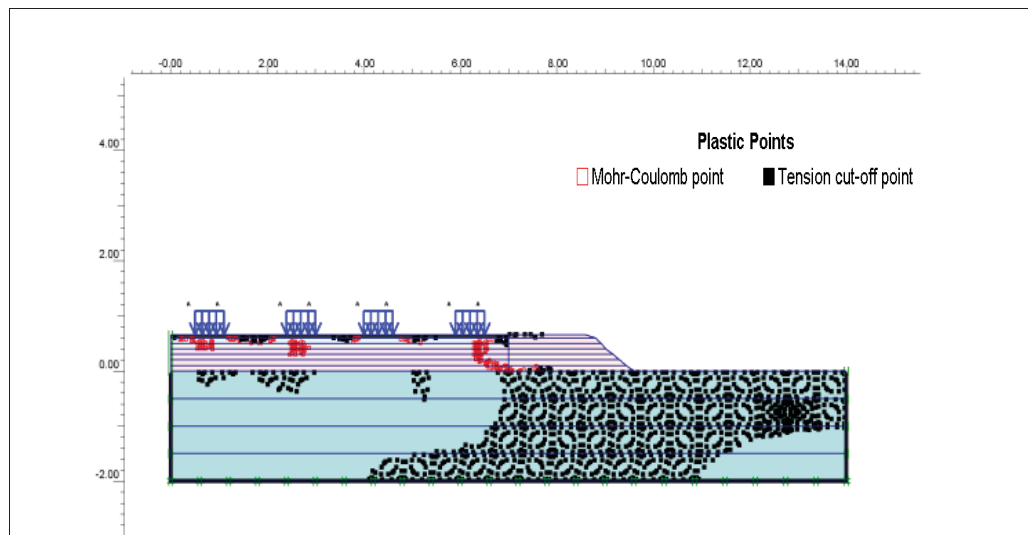
Mohr-Coulomb model

Soft-Soil model

Figure 7. Plastic, tension-cut-off and Cap points

a- Linear elastic model
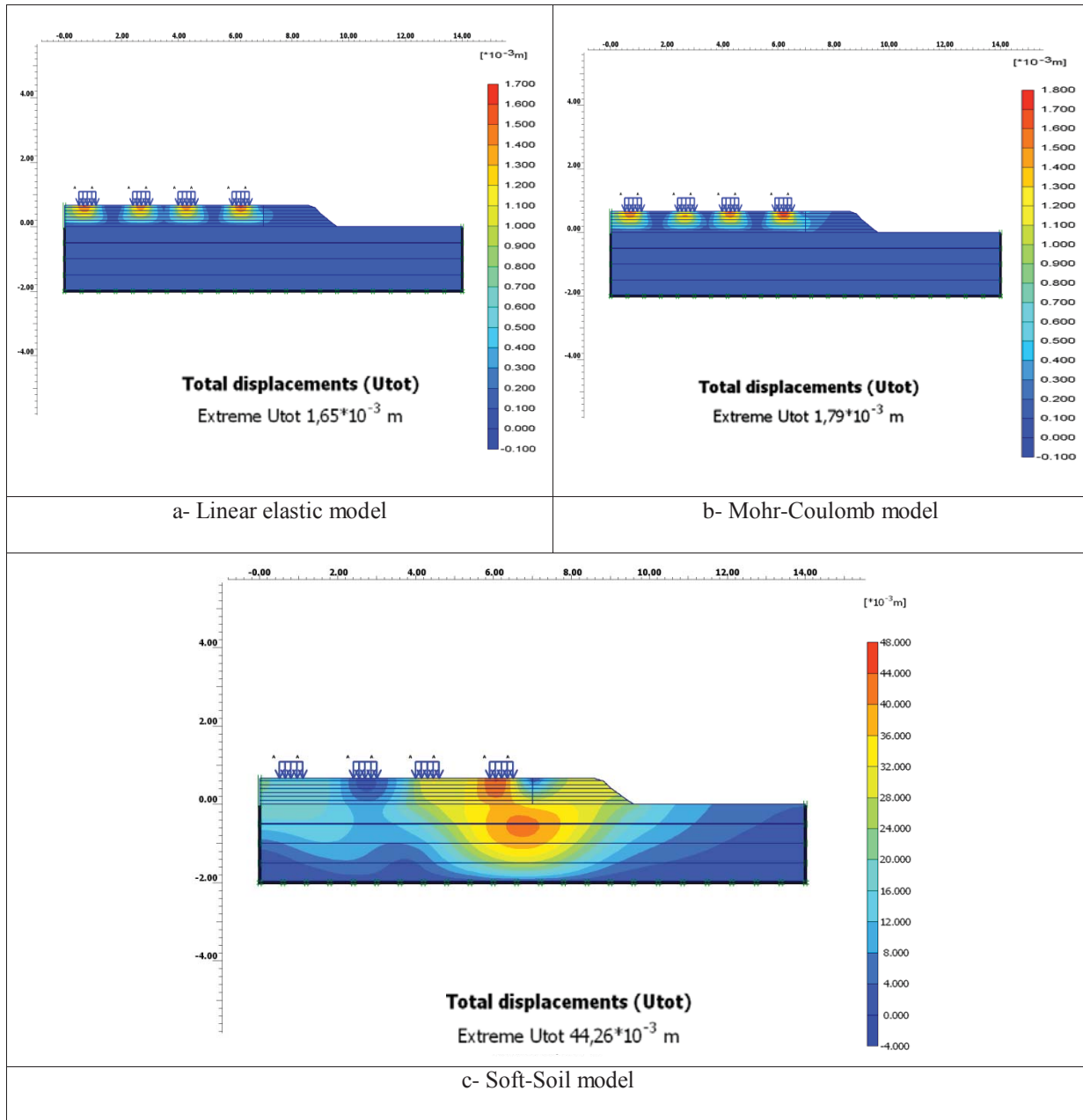
b- Mohr-Coulomb model

c- Soft-Soil model

Figure 8. Total displacements

variation in pavement will diminish. The subgrade soil is over-excavated in the seasonal active zone to a depth where the moisture content remains virtually constant over time leading the volume change of the soil to be negligible over time.

The swelling pressure was determined by the oedometer test, and after simulation, it output the value of 240 kN/m2. The surcharge pressure must be the same in order to avoid the height settlements. Calculation of surcharge pressure was based on a method introduced

by Terzaghi [1954]. When computing the surcharge fill properties, non-traffic load conditions was considered with the purpose of stabilizing the swelling pressure.

$$\sigma_Z = \frac{P_p}{S} \qquad (4)$$

$$\sigma_Z = \gamma_a \times H_L \qquad (5)$$

Then
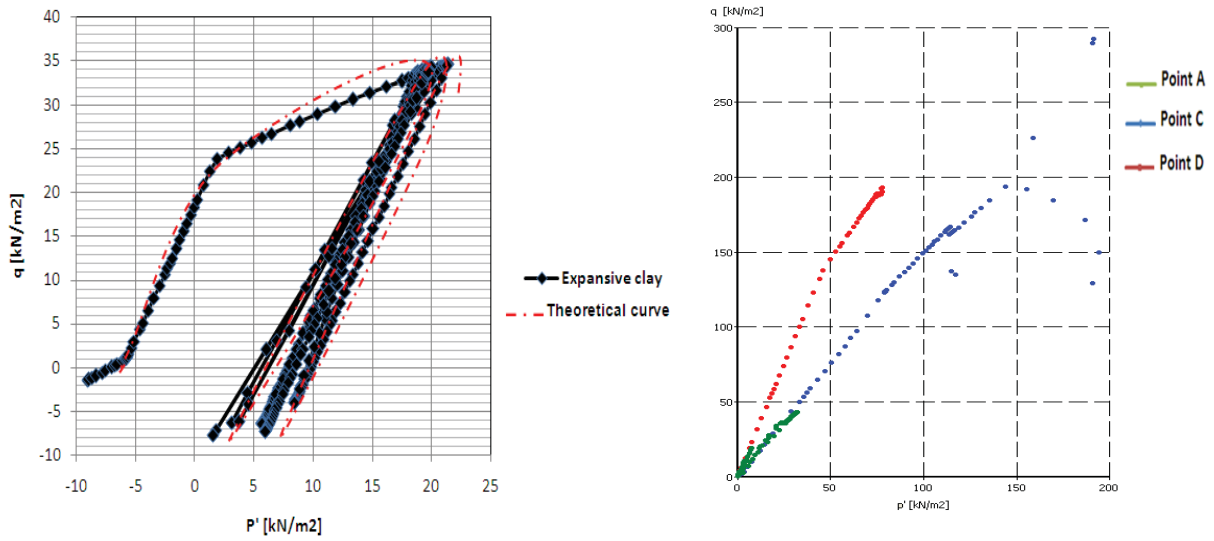$$P_P = \gamma_a \times H_L \times S \qquad (6)$$

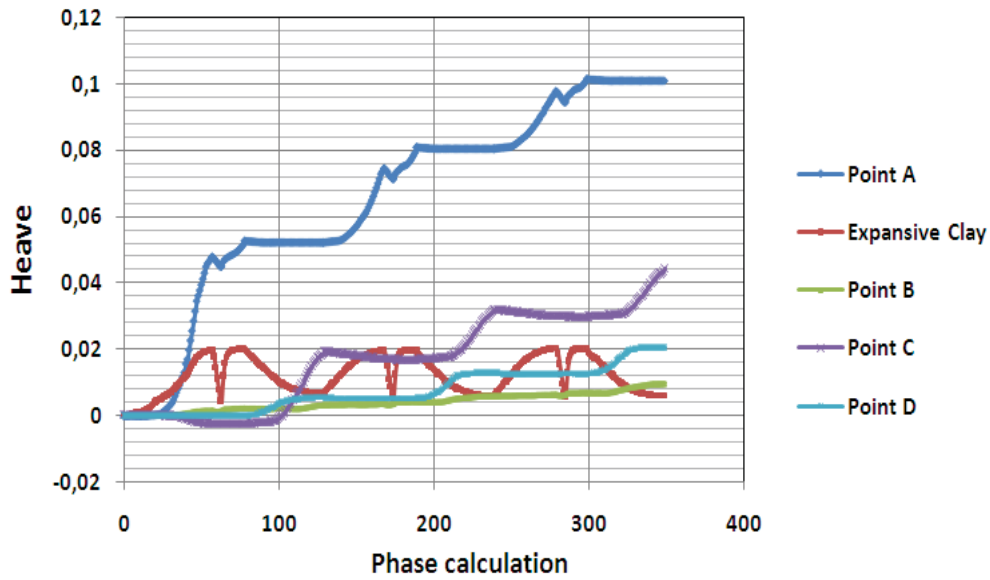**Figure 9. Stress path; left: subgrade, right: pavement structure.**

Figure 10. Vertical displacement of pavement and subgrade
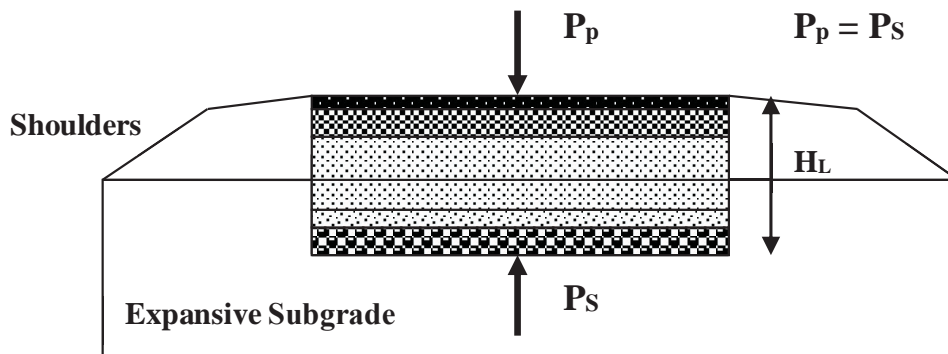

Figure 11. The principle of the stabilization of an expansive subgrade

where P_p is the applied vertical pressure [kN/m2], γ_a the average total density of the fill [kN/m3], HL is the selected fill thickness [m] and S is the area of the fill soil which is assumed as square of each side 1 m.

Calculation resulted in a total thickness of the surcharge layer of 1.1 m. The fill layer is designed including 0.40 m layer of ballast to limit the capillarity ascension, 0.10 m layer of crushed sand as anti-contamination layer, 0.40m of layer of calcareous tufa as embankment, 0.20 m layer of crushed gravel as base course and 0.06m asphalt on the top. The earthmoving operation started in July 2007, when the precipitation is rare and the temperature reaches to 45°C. The purpose was to reduce the variation of moisture content. During the construction of the fill and after five years of service, the variation of heave of pavement versus the time has been plotted in Figure. 12. The Figure shows that, prior to the fill, the heave of the subgrade had been 0.023 m as the maximum recorded expansion. Later, it decreases to -0.005 m at the end of the first month of the treatment. After nine months, the settlements are almost stabilized at -0.007 m with no cracks in pavement. Moreover, after three years the maximum settlement reaches -0.009 m due the secondary consolidation with no deformation in the pavement structure.

7. Conclusions

This study is focused on determination of the behavior of flexible pavements under the influence of the evolutionary character of swelling soils of Tebessa, Alge-

ria. Based on the results reported in this study, we can concluded that the subgrade soils of the study area are marly clays with 64% of calcite and 35% of aluminosilicate having medium to high Atterberg limits, medium to high swell potential and high swelling pressure about 350 kN/m2.

The surprising distribution of permanent deformations in this model shows that it is not easy to predict where deformation will occur. For similar loading conditions, it is clear that the explanation of the permanent strain distribution can only be found through the relations between the stresses and stiffness of the materials [i.e. material properties and their thickness]. The calculations indicate that with linear elastic model, the deformations concentrated exclusively in the pavement depend on the traffic load, which limits the damage only in these areas with zero plastic deformations. Therefore, this model is a suitable one used for designing pavement structures with a deformation of about 1.65×10^{-3}m.

Mohr-Coulomb model reveals that the deformations are concentrated exclusively in the pavement situated in direct contact with traffic loads, with the appearance of tension cut-off points in the surface course, subgrade side shoulder and the surrounding area of the structure pavement. It indicates there is a cracks network in these areas due to the shrinkage of the clayey soil inducing cracking in the pavement. The deformation is near the linear elastic model with 1.76×10^{-3} m. In Soft-Soil model, the permanent deformations are not the identi-
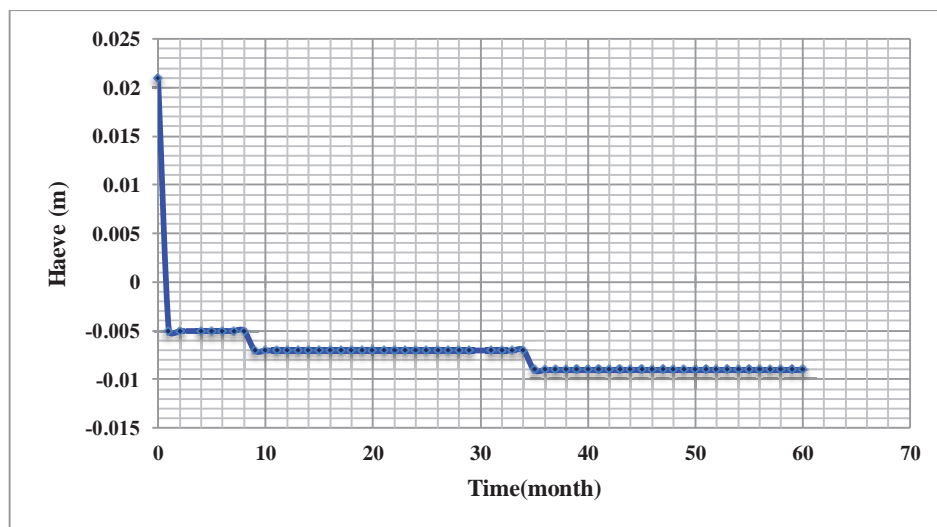

Figure 12. Variation of heave of pavement versus the time

cal throughout the structure. The model shows that the majority of displacements are in the shoulder side of the subgrade, which indicates that the source of displacements is the transitional subgrade between the pavement and its shoulder. These distortions arise mainly at first by the swelling subgrade, and secondly by the application of traffic load. Their value is 44.26×10^{-3} m, which creates an influence zone that spreads to the shoulders and the surrounding area of the pavement structure.

Deformations are confirmed by plastic points where the cup points are manifested in the subgrade along the shoulders and in the middle of the pavement, which indicate that the stress state in these points is equivalent to the pre-consolidation stress or they are highly loaded to the maximum stress level that has previously been reached. Hence, the pavement is solicited by both sides; traffic which transmits a high pressure to subgrade and to groundwater, and deformations caused by the expansion of subgrade. Along the shoulders, there is a concentration of tension cut-off points. The points are in failure state under tensile stress, which explains the appearance of crack networks along the shoulders. The cracks promote water penetration to the pavement structure creating a zone of saturation that will reduce the bearing capacity of the soil, decrease the stability of the shoulder slope, and produce settlement and lateral displacement of shoulder. Coulomb plastic points concentrated in the contact zones of traffic indicate where the Mohr's stress circle touches the Coulomb failure envelope. Therefore, it limits the state of failure along the shoulders; thus, imbalance area is created.

It is also found that the subgrade has a hardening behavior, i.e. elasto plastic type of hyperbolic model. The soil deforms according to the charge induced by traffic with an increase in the plasticity limit, then, the amplification of the surface load. This behavior affects considerably the deformation in different parts of the pavement where deformations are not identical in its different parts.

These observations accord fairly with Laroche's work [1973], which describes perfectly the behavior of flexible pavements over expansive soils and conform perfectly to the results of this research. Therefore, deterioration taking place in the subject road is not caused only by the traffic load but rather by the slow cyclic variation of swelling soil. The soft soils generate large strains as

function of the magnitude of external loads where the results adapt perfectly with the Soft-Soils model.

Stabilization of cyclic movements of expansive subgrade is neutralized by applying surcharge equal to the swelling pressure. This is done by applying surcharge fill pressure equal to the swelling pressure. The application of the surcharge fill has reached the value of -0.005 m at the end of the first month. After nine months, the settlements had been stabilized with -0.007 m of deformation and no cracking in the pavement. Moreover, after three years, the settlements increase just slightly to -0.009 m due the secondary consolidation in the pavement structure.

8. Acknowledgement

9. References
- Ayman, A. (2007) "Numerical simulation of a trial wall on expansive soil in Sudan", Plaxis Bulletin issue 21

- Baheddi, M., Djafarov, M. and Charif, A. (2007) "Design method of flexible continuous footing on swelling clayey soils", Medwell journals, Journal of engineering and applied sciences, 2[3], pp.531-539

- Banu, S., Mustafa, A., Mustafa, V. and Fikret, K. (2009) "Prediction of swelling pressures of expansive soils using artificial neural networks". Elsevier Scientific Publishing, Advances in Engineering Software, 41,pp 647–655

- Brinkgreve, R.B.J. (2003) "Reference Manual Plaxis2D", Delft University of Technology & PLAXIS bv, Netherlands.

- Brinkgreve, R.B.J. (2003) "Material Models Plaxis2D", Delft University of Technology & PLAXIS bv, Netherlands.

- Bultel, F. (2001) « Prise en compte du gonflement des terrains pour le dimensionnement des revêtements des

tunnels », Thèse de Doctorat, école nationale des ponts et chaussées, Paris [in french].

- Chen, F.H. (1988) "Foundations on Expansive Soils", Elsevier Pub Co, Amsterdam

- Dakshanamanthy, V. and Raman, V. (1973) "A Simple Method of Identifying an Expansive soil", Soils and Foundations, Japanese Society of Soil Mechanics and Foundation Engineering, 13 [1], pp 97–104

- Duhamel, D., Nguyen, V., Chabot, A and Tamagny, P. (2003) « Modélisation de chaussées viscoélastiques ». 16ème Congrès Français de Mécanique, Nice, pp 1-5 [in french].

- Felt, E.J. [1953] "Influence of Vegetation on Soli Moisture Content and Résultent Soil Volume Changes.", Proceedings of 3rd Conference on SMFE, Vol 1, Zurich

- Gupta, R., McCartney, J. S., Nogueira, C. L and Zornberg, J. G. (2008) "Moisture Migration in Geogrid Reinforced Expansive Subgrades", The First Pan American Geosynthetics Conference & Exhibition, Cancun, Mexico

- Hyunwook, K. and William, G. (2009) "Finite element cohesive fracture modeling of aairport pavements at low temperatures", Elsevier Scientific Publishing, Cold Regions Science and Technology, 57, pp 123–130

- Işık, Y. [2006] "Indirect Estimation of the Swelling Percent and a New Classification of Soils Depending on Liquid Limit and Caption Exchange Capacity", Elsevier Scientific Publishing, Engineering Geology ,85, pp 295–301

- Jones, D.E. and Holtz, W.G. (1973) "Expansive Soils-the Hidden Disaster", Civil Engineering, Vol. 43, No. 8

- Laroche, C. (1973) «" Étude des sols pour la route Waza Maltam, Sur Argile Gonflante ». Revue générale des routes n° 486 [in french]

- Leena, K. and Rainer, L. (2004) "Modelling of the stress state and deformations of APT tests". VTT Technical Research Centre of Finland. In: Proc. of the 2nd International Conference on Accelerated Pavement Testing.

- Lianheng, Z., Liang, L., Feng, Y. and Jing, Z.(2010) "Evaluating the Effects of the Magnitude of Pseudostatic Force on Reinforced Slopes based on the Nonlinear M-C Failure Criterion", EJGE, Vol. 15, Bund. J, pp1017-1052

- Marienfeld, M.L. and Baker, T.L. (1999) "Paving Fabric Interlayer as a Pavement Moisture Barrier", Transportation Research Circular, E-C006

- Miura, N., Sakai, A., Taesiri, Y., Yamanouchi, T. and Yasuhara, K. (2003) "Polymer grid reinforced pavement on soft clay grounds", Elsevier Scientific Publishing, Resources, Geotextiles and Geomembranes, volume 9, Issue 1, 1990, pp 99–123

- Prasad, D.S.V., Kumar, M. and PrasadaRaju, G.V.R. (2010) "Behavior of reinforced sub bases on expansive soil subgrade, Global Journal of Researches in Engineering, Vol. 10 Issue 1,Ver 1.0

- RamanaMurty, V. (1998) "Study on swell pressure and the method of controlling swell of expansive soil", Ph.D. Thesis, Kakatiya University, REC, Warangal,A.P.

- Saad, A. and Aiban. A. (2006) "Compressibility and swelling characteristics of al-khobar palygorskite, eastern Saudi Arabia", Elsevier Scientific Publishing, Engineering Geology 87, pp 205–219

- Snethen (1975) "Review of engineering experiences with expansive soils in highway subgrades", US Army Engineer Water Ways Experiment Station, FHWA, USA

- Steinberg, M.L. (1977) "Ponding an Expansive Clay Cut: Evaluations and Zones of Activity", TRR-641, TRB, pp 61-66

- SubaRaob, K.S. and Satyadas, G.C. (1980) "Prewetted and Overloaded Expansive Soil", Proceedings of

Geotech. 80, Bombay, pp 29-32

- Terzaghi, K. (1954) "Anchored Bulkheads", Transactions, ASCE, 119

- Thompson, M.R. and Robnett, Q.L. (1976) "Pressure Injected Lime for Treatment of Swelling Soils". One of the 4 reports Prepared for the 54th Annual meeting of the TRB, TRR-568, pp 24-34

- Žlender, B. (2008) "Prediction of permanent deformation of pavement's unbounded layers based on cyclic triaxial tests", American Journal of Applied Sciences, 5 [1], pp 22-28

- Zornberg, J.G., Gupta, R., and Prozzi, J. (2009) "Geogrid Reinforcement of Pavements over Expansive Clay Subgrades", Proceedings of the 17th International Conference on Soil Mechanics and Geotechnical Engineering.doi:10.3233/978-1-60750-031-5-765

- Available online: < http://maps.google.fr/>.